Fractographic Investigation on Root Crack in the TRC Test of HY-130 Steel†

— Studies on Fractography of Welded Zone (II) —

Fukuhisa MATSUDA*, Hiroji NAKAGAWA, Kenji SHINOZAKI***, Hiroshi KIHARA****, Soutaro YAMADA*****, Yoshinari IWAMURA*****, Yuji OHKUMA***** and Jinichi SHIMOYAMA********

Abstract

The clue of the weld cracking of HY-130 has been explored by observing the fracture surface of the root crack of HY-130, HY-90 and HY-110 undergone the TRC test with a scanning electron microscope. Main conclusions obtained are as follows: (1) *The whole of the fracture surface consists of three or four characteristic fracture regions.* (2) *The distribution of the each characteristic fracture region depends on the kind of the base metal, the applied stress in the TRC test, the preheating temperature and the welding procedure.* (3) *The root crack of HY-130 with SMA welding predominantly propagates through the weld metal and contains a large quantity of intergranular fracture region in the lowest applied stress. Therefore the major problem of the weld cracking of HY-130 exists in the weld metal.* (4) *The root crack of HY-130 with SMA welding mainly consists of hydrogen-induced crack, though there are few micro solidification cracks.* (5) *Dimple fracture region is formed by an unstable crack propagation and a linear fracture mechanics can be approximately applied to the fracture.*

1. Introduction

Because welded steel structures are gradually used in severer environments and conditions, and because lighter weight structures are demanded from an economical viewpoint etc, the development of steels of high strength and of good toughness in low temperatures has been desired.

The HY steels have been developed in order to satisfy the above demands, and HY-80～HY-110 have been already put to practical use.

However, it is known that HY-130 (5Ni-Cr-Mo) has high susceptibility to the weld cracking, and the delayed crack in the weld metal[1,2] is regarded as important together with that in the heat-affected zone[3-5] On the other hand it is reported[6] that HY steel has high susceptibility to solidification crack according to its nickel and carbon contents. Moreover, there is an opinion[7] that a micro hot crack has a possibility to grow into a large delayed crack in a high strength steel such as HY steel. However, there is not a clear evidence to prove or to deny this opinion, although there is a report[8] which shows a negative conclusion for HY-80. While, Savage et al.[9] showed that the hot crack in HY-80 occurred not in the heat-affected zone but in the unmixed zone.

Judging from the above mentions, in HY-130 higher than HY-80 in strength there remains a possibility that a micro solidification crack grows into a large delayed crack in the weld metal. Therefore it can not be understood whether the basic cause to the weld cracking of HY-130 is a solidification crack, a plain delayed crack, or another unknown crack.

Thus, in this report the clue of the weld cracking of HY-130 has been explored by observing in detail the fracture surface of root crack of HY-130 undergone the TRC test[10] with a scanning electron microscope.

2. Materials Used and Experimental Procedures

2.1 Materials Used

Chemical compositions of base metals used and deposited metals made from welding rods used are summarized in **Table 1.** Two heats of HY-130 were prepared, and one was expressed as HY-130 (E) and the other as HY-130 (F). Moreover, HY-90 and HY-110 steels were used together with HY-130 steels in order to compare the fracture characteristic each other. As welding rods, E130A and E130B※ for HY-130 (E), E90 for HY-90, and E110 for HY-110 were used, where the symbol E designates that it is an electrode used for shielded metal-arc (SMA) welding. For HY-130 (F), F130 was used, where the symbol F designates that it is a filler metal used for gas tungsten-arc (GTA) welding with an automatic wire feeder.

† Received on November 1, 1977

* Professor
** Research Instructor
*** Graduate Student
**** Honorary Professor of Tokyo and Osaka Universities
***** Kawasaki Heavy Industries Co. LTD
****** Mitsubishi Heavy Industries Co. LTD

※ Electrodes E130A and E130B were used only for expreimental purpose and are not practically used at the present.

Table 1 Chemical compositions of base metals and deposited metals

Material		Thickness (mm)	Diameter (mm)	Composition									
				C	Si	Mn	P	S	Cu	Ni	Cr	Mo	V
Base metal	HY-130(E)	40	–	0.09	0.29	0.49	0.005	0.004	0.05	5.32	0.51	0.53	–
	HY-130(F)	65	–	0.09	0.27	0.83	0.006	0.0012	0.02	5.20	0.50	0.53	0.055
	HY-90	38	–	0.11	0.26	0.57	0.009	0.007	0.07	2.90	0.71	0.37	tr.
	HY-110	40	–	0.06	0.25	0.67	0.004	0.005	0.02	3.95	0.61	0.48	0.06
Welding rod	E130A	–	4	0.05	0.37	1.45	0.007	0.004	–	2.67	0.95	0.59	–
	E130B	–	4	0.05	0.53	1.11	0.004	0.007	0.15	3.28	0.48	0.84	–
	F130	–	2.4	0.10	0.29	1.65	0.011	0.010	–	3.50	0.97	1.23	–
	E90	–	4	0.06	0.42	0.93	0.011	0.004	0.04	2.71	–	0.30	–
	E110	–	4	0.05	0.41	1.38	0.008	0.004	–	2.65	0.80	0.57	–

Table 2 Mechanical properties of base metals and deposited metals

Material		Yield strength (0.2% offset) (kg/mm^2)	Tensile strength (kg/mm^2)	Elongation (%)	Charpy V-notch energy absorption (kg-m)		
					0(℃)	−50(℃)	−70(℃)
Base metal	HY-130(E)	96.9	102.4	21.0	26.0	–	25.0
	HY-130(F)	94.0	101.7	23.5	21.0	–	20.4
	HY-90	65.0	75.0	26.5	25.3	–	24.3
	HY-110	83.0	90.0	23.0	24.2	–	25.7
Welding rod	E130A	94.9	99.6	19.3	7.6	5.0	–
	E130B	93.5	97.5	19.9	7.8	5.3	–
	F130	99.2	104.6	21.5	15.0	13.1	–
	E90	65.1	74.9	25.7	19.6	13.7	–
	E110	89.4	93.9	19.3	8.2	5.2	–

Table 3 Preheating temperature in the TRC test

Combination	Preheating temperature (℃)
HY-130(E)+E130A	R.T.*, 75, 150
HY-130(E)+E130B	75
HY-130(F)+F130	75,100,150
HY-90+E90	R.T.*
HY-110+E110	75

*Room temperature

Their mechanical properties are shown in **Table 2.** The yield strength and the tensile strength of each deposited metal well match those of the corresponding base metal.

2.2 The TRC Test

The TRC testing machine consists of a 100-ton tensile testing machine placed horizontally. Prior to the test, the electrode for SMA welding was dried for 1 hr. at 400°C, and then the diffusible hydrogen content obtained with. JIS* method using glycerine was about 1 ml/100 g. The weld bead of about 120 mm length was deposited in a *y*-slit groove of base metal with the weld heat input of 17000 J/cm at room temperature or at a preheated temperature. The preheating temperature was selected as shown in **Table 3.** The tensile restraint stress was applied immediately after the welding, and the set stress of the tensile restraint was obtained within one minute. The maximum testing time was limited to two days.

2.3 Observation of Fracture Surface

The macroscopic feature of fracture surface of the TRC test specimen was observed with the naked eye, and then the microscopic feature was observed in detail with a scanning electron microscope (SEM). If need were, the element on the fracture surface was analyzed with an energy dispersive-type analyzer (EDX) attached to the SEM. As mentioned later, the SEM observation revealed an intergranular fracture region, quasi-cleavage fracture region and etc, and each frac-

* JIS: Japan Industrial Standard.

ture region shows its macroscopically peculiar feature which can be discriminated on a light fractograph of about ten magnification. Therefore the area fraction of each fracture region occupied in the whole of the fracture surface was measured with a planimeter on the light fractograph.

3. Experimental Results

3.1 Effect of Applied Stress on Fracture Time

The relation between applied stress and fracture time in the TRC test is summarized in **Fig. 1.** The comparison between the combination of HY-130 (E) plus E130A at room temperature and that of HY-90 plus E90 at room temperature or the comparison between the combination of HY-130 (E) plus E130A at 75°C and that of HY-110 plus E110 at 75°C suggests that HY-130 has an extremely high tendency for weld crack, although the combination of HY-130 (E) plus E130B is somewhat preferable to that of HY-130 (E) plus E130A. However, it is noteworthy that HY-130 is comparatively superior in GTA welding. That is, the lower critical stress in the combination of HY-130 (F) plus F130 at 75°C is about 85 kg/mm² in constrast with about 25 kg/mm² in the combination of HY-130 (E) plus E130A at 75°C.

Besides, the fact that the increase in the preheating temperature raises the lower critical stress in the combination of HY-130 (E) plus E130A suggests that the weld cracking of HY-130 in the TRC test mainly consists of hydrogen-induced delayed cracking.

3.2 Macroscopic Feature of Root Crack Path in Transverse Cross Section

The macroscopic feature of the root crack of HY-130 in the transverse cross section is that the crack predominantly passes through only the weld metal regardless of applied stress and of welding procedure as shown in **Photo. 1(a), (b)** and **(c)**. Therefore it is supposed that in HY-130 the crack susceptibility of the weld metal is more important than that of the heat-affected zone.

On the other hand, the macroscopic feature of the root crack of HY-90 is that the crack passes through both the heat-affected zone and the weld metal as shown in **Photo. 1(d),** although at a higher applied stress the crack frequently passes through only the weld metal as shown in **Photo. 1(e).** Though the reason for these phenomena should be mentioned later, it is supposed that in HY-90 the crack susceptibility of the heat-affected zone is more important than that of the weld metal. By the way, the crack path in Photo. 1(d) is similar to that of usual constractional high strength steel undergone the Tekken *y*-slit groove test[11].

In HY-110, the majority of the crack path is similar to that of HY-90, but the crack path similar to that of HY-130 is also observed as shown in **Photo. 1(f).**

3.3 Microscopic Feature of Fracture Surface

The detailed observation of all over the fracture surfaces with SEM revealed that whole of the fracture surface consists of three or four fracture regions among IG_c, QC, QC_c, CD_c and D regions which were de-

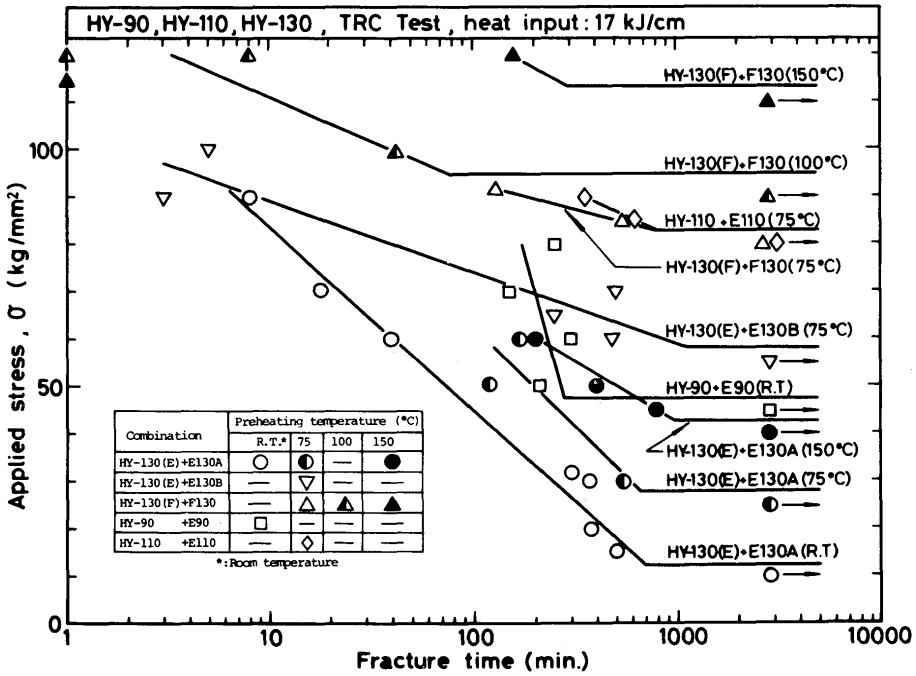

Fig. 1 Relation between applied stress and fracture time

(a) HY-130(E) plus E130A, applied stress $\sigma=15$ kg/mm², without preheating

(b) HY-130(E) plus E130A, $\sigma=90$ kg/mm², without preheating

(c) HY-130(F) plus F130, $\sigma=85$ kg/mm², preheating temperature $T_p=75$ °C

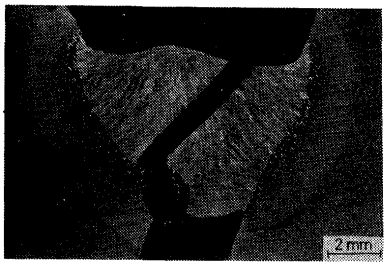

(d) HY-90 plus E90, $\sigma=50$ kg/mm², without preheating

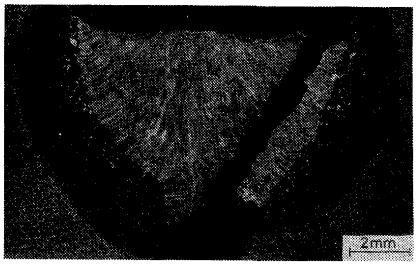

(e) HY-90 plus E90, $\sigma=90$ kg/mm², without preheating

(f) HY-110 plus E110, $\sigma=85$ kg/mm², $T_p=75$ °C

Photo. 1 Macrophotograph of transverse cross section of TRC test speicmen

nominated by the authors.

3.3.1 *IG_c Region*

The designation IG_c is an abbreviation of intergranular fracture along columnar crystal boundary of prior austenite. The fracture surface of IG_c region macroscopically has a directional appearance and gives a brilliant impression, as seen in Photos. 10 and 11 lately mentioned.

The microfractograph of IG_c region in a low magnification, **Photo. 2(a),** shows a large portion of smooth surface and a small portion of rough surface. The smooth portion is magnified in **Photo. 2(b),** which shows intergranular fracture along the columnar crystal boundary of the prior austenite in the weld metal. Many voids, hairlines and occasional dimples are seen on the fracture surface, which suggest an existence of some plastic deformation at the fracture. Inclusions are often observed in these voids and dimples as shown in **Photo. 2(c),** and the EDX result, **Photo. 2(d)**, shows existences of Si, Al, Ti and Mn in the combination of HY-130 (E) plus E130A. Occasionally Cr and S were also detected.

The rough portion of Photo. 2(a) consists of quasi-cleavage fracture surface or dimple fracture surface as a transgranular fracture. An example of the quasi-cleavage fracture surface is shown in **Photo. 2(e),** which is different from that resulted from brittle fracture in a low temperature and thus is considered to be resulted from hydrogen embrittlement. This fracture surface also suggests some plastic deformation, judging from existences of many tear ridges and voids. Thus the IG_c region above defined contains a small portion of the transgranular fracture such as the quasi-cleavage and the dimple fractures in addition to the pure intergranular fracture.

By the way, estimating from the contour of IG_c region of HY-130 or HY-110 shown in Photos. 10, 11 and 14 lately mentioned, the IG_c region seems to propagate as a fan-like shape from a pivot situated at the root edge which corresponds to the crack-initiated part. On the other hand, it is well known[12-14] that hydrogen-induced crack occurs intergranulary in the lowest stress intensity factor. In the TRC test, the stress intensity factor becomes larger as the crack propagates, because the applied load is constant. Therefore the above mentioned pivot part is considered to be the crack initiation point for the whole of the root crack. Therefore the elucidation of the fracture mode at the pivot part is considered to be a key to solve the basic cause for the weld cracking of HY-130. For that reason the fracture surfaces of seventeen pivot parts of IG_c regions of the combination of HY130 (E) plus E130A are investigated in detail.

The general appearance of the fracture surface near the pivot part is shown in **Photo. 3,** where the lowest end is the root edge and the part of a mark S is the pivot part. The fracture mode at the vicinity of the

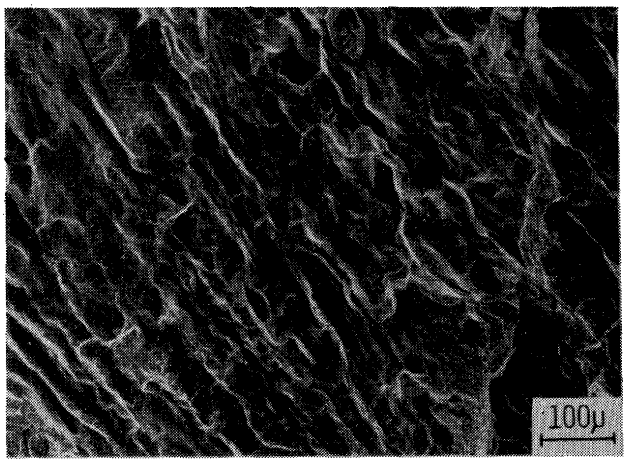

(a) lower magnification

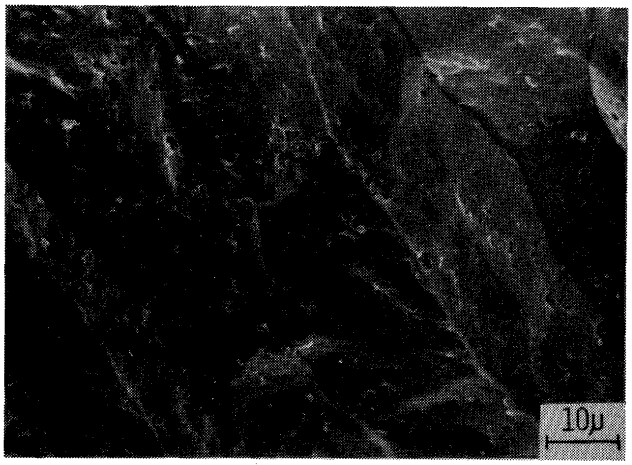

(b) typical example in higher magnification

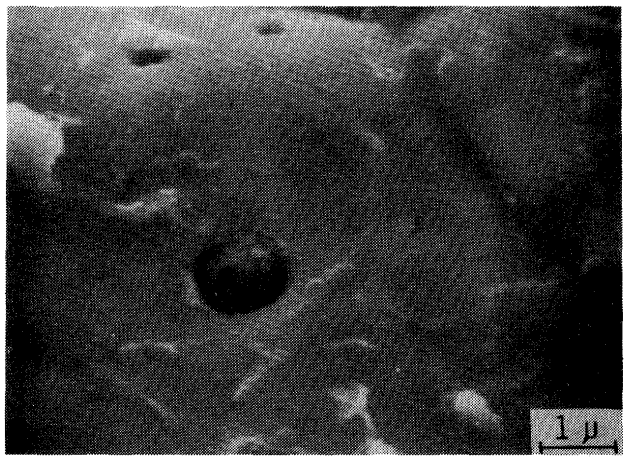

(c) inclusion on intergranular fracture surface

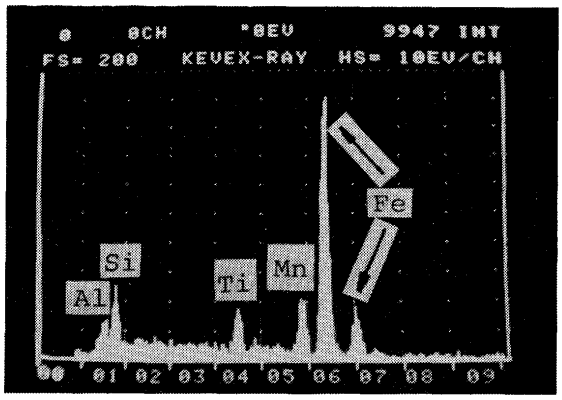

(d) EDX result of the inclusion in (c)

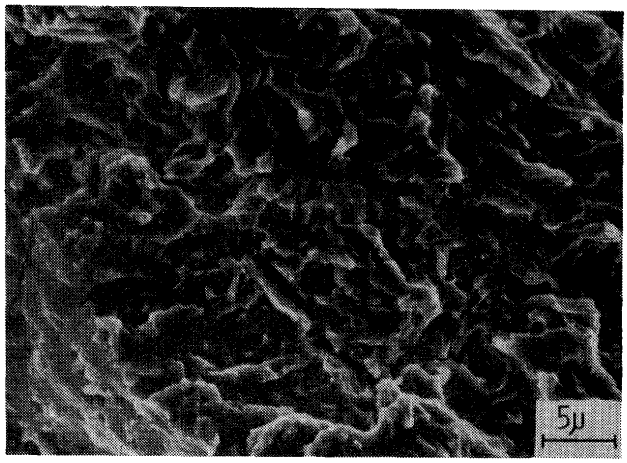

(e) quasi-cleavage fracture part

Photo. 2 Microfractograph of IG_c region, HY-130(E) plus E130A, $\sigma=15$ kg/mm², without preheating

mark S is essentially identical with that in Photo. 2(a). However, fracture surfaces resulted from solidification crack were observed at only two among seventeen pivot parts. One example is shown in **Photo. 4,** where a solidification crack is observed in the outlined area. The fracture surface in a higher magnification, **Photo. 5,** shows a dendritic feature. This certainly corresponds to a micro hot crack which grew into a delayed cracking. However, there was no micro solidification crack in the specimen of the lowercritical stress ($\sigma=15$kg/mm²). Therefore it will be concluded that the micro solidification crack is not the basic cause of the weld cracking of HY-130.

3.3.2 *QC_c Region*

The designation QC_c is an abbreviation of quasi-cleavage fracture which has a directional appearance

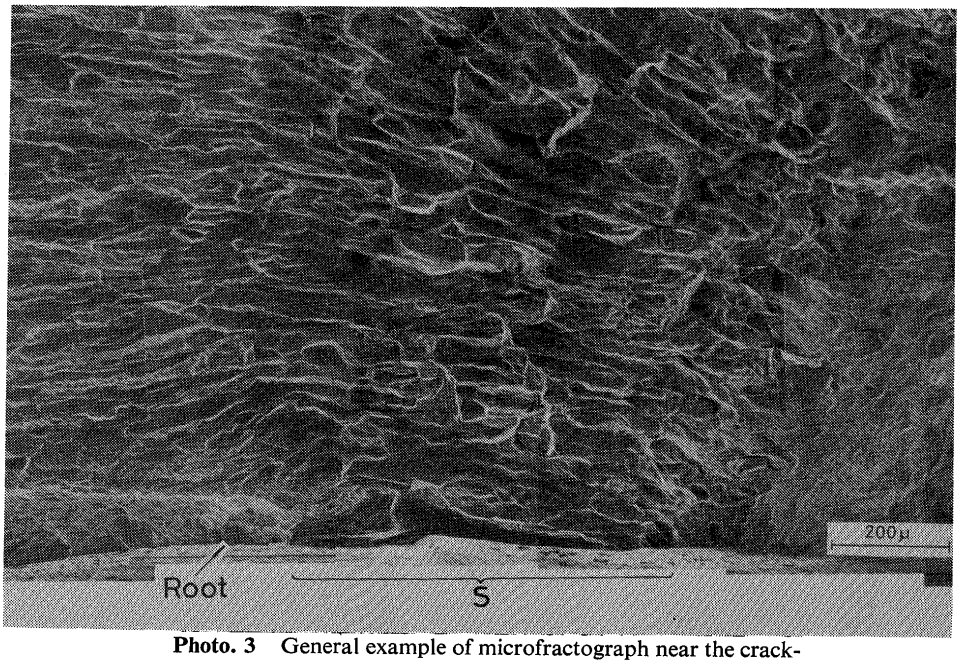

Photo. 3 General example of microfractograph near the crack-initiated part of IG_c region, HY-130(E) plus E130A, $\sigma=15$ kg/mm², without preheating

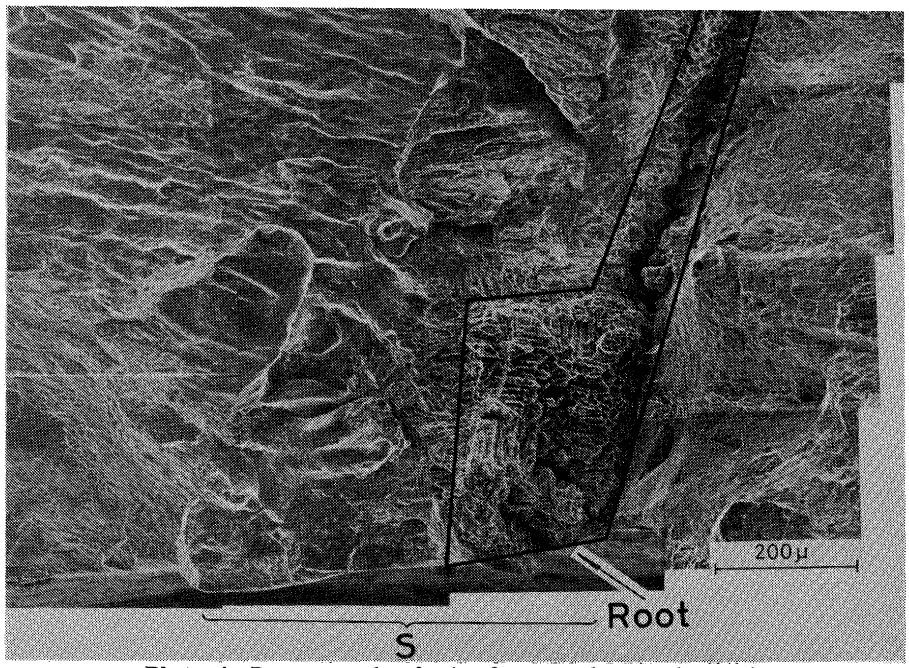

Photo. 4 Rare example of microfractograph near the crack-initiated part of IG_c region, HY-130(E) plus E130A, $\sigma=20$ kg/mm², without preheating

owing to the columnar crystals of prior austenite in the weld metal. This QC_c region was observed only in the combination of HY-130 (F) plus F130 with GTA welding.

The microfractograph of QC_c region in a low magnification is shown in **Photo. 6(a),** where the fracture surface more than half is occupied by the quasi-cleavage fracture having a directional appearance and the remaining portion, which is located at the center in Photo. 6(a), is occupied by the intergranular fracture similar to that in the IG_c region. The quasi-cleavage fracture surface is magnified in **Photo. 6(b),** which also considered to be resulted from hydrogen embrittlement and is similar to that in Photo. 2(e) except for the appearance of somewhat smaller plastic deformation. The intergranular fracture surface is magnified

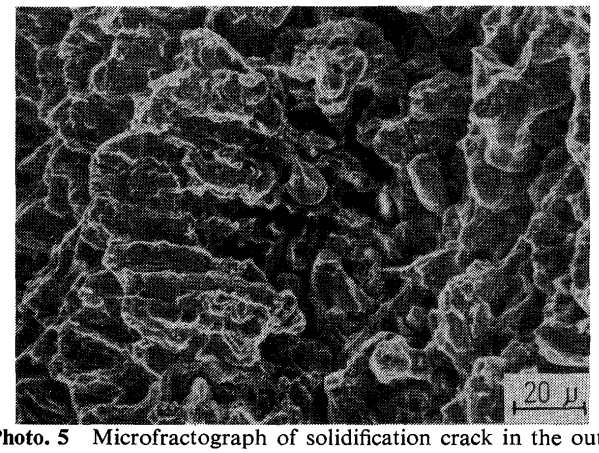

Photo. 5 Microfractograph of solidification crack in the outlined area in Photo. 4

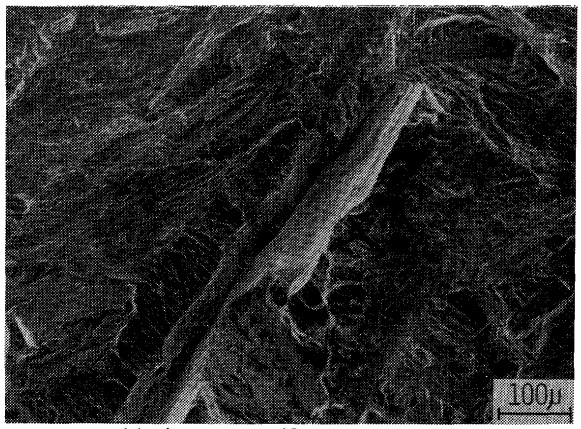

(a) lower magnification

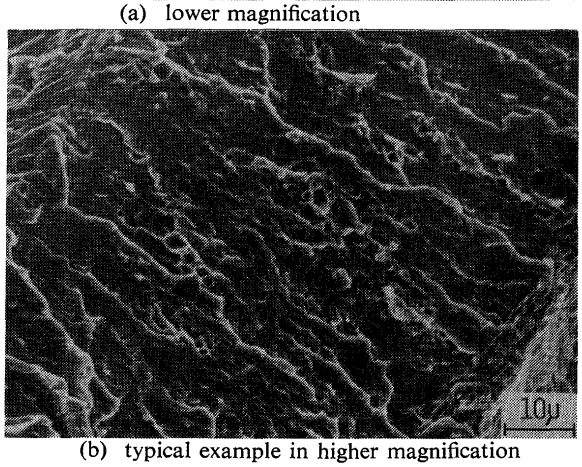

(b) typical example in higher magnification

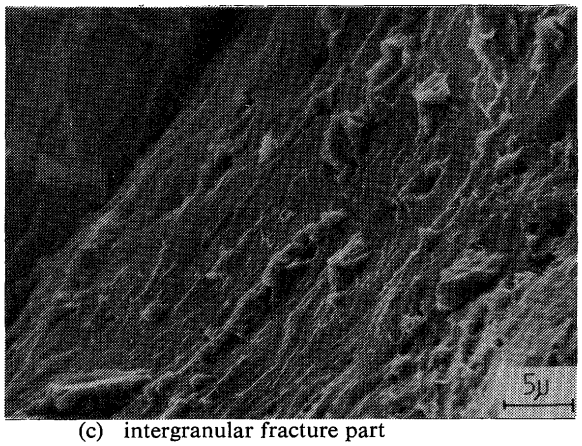

(c) intergranular fracture part

Photo. 6 Microfractograph of QC_c region, HY-130(F) plus F130, $\sigma=92$ kg/mm^2, $T_p=75$°C

in **Photo. 6(c)**, where many hair lines are observed.

3.3.3 *CD_c Region*

The designation CD_c is an abbreviation of quasi-cleavage plus dimple fracture which has a directional appearance owing to the columnar crystals of prior austenite in the weld metal. Macroscopically the fracture surface of the CD_c region gives a slightly brilliant impression.

The microfractograph of CD_c region is shown in **Photo. 7(a)** in a low magnification, whose appearance is approximately even. The microfractograph in a higher magnification, **Photo. 7(b),** shows intermingled fracture mode of terraced quasi-cleavage fracture and dimple fracture, which may suggest that the CD_c region is a transient region from quasi-cleavage fracture to dimple fracture. This CD_c region is also considered to be resulted from hydrogen embrittlement. Therefore it is considered that the CD_c region is formed in a higher stress intensity factor than that in the IG_c region. Namely, the CD_c region may be formed later than the IG_c region.

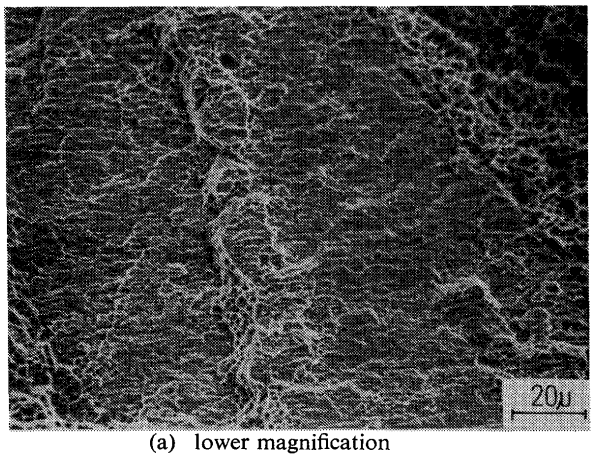

(a) lower magnification

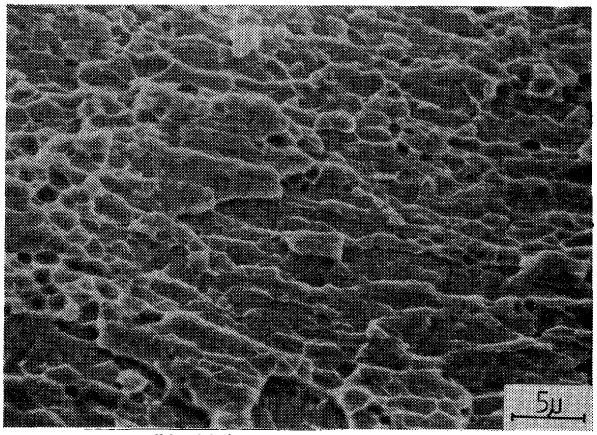

(b) higher magnification

Photo. 7 Microfractograph of CD_c region, HY-130(E) plus E130B, $\sigma=90$ kg/mm^2, $T_p=75$°C

3.3.4 *QC Region*

The designation QC is an abbreviation of quasi-cleavage fracture in the heat-affected zone. The fracture surface of the QC region macroscopically gives a brilliant impression, but has not a directional appearance. The general microfractograph of the QC region is shown in **Photo. 8(a),** where tear ridges

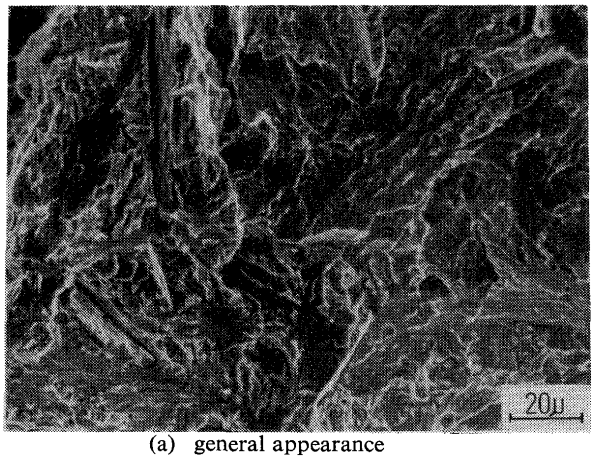

(a) general appearance

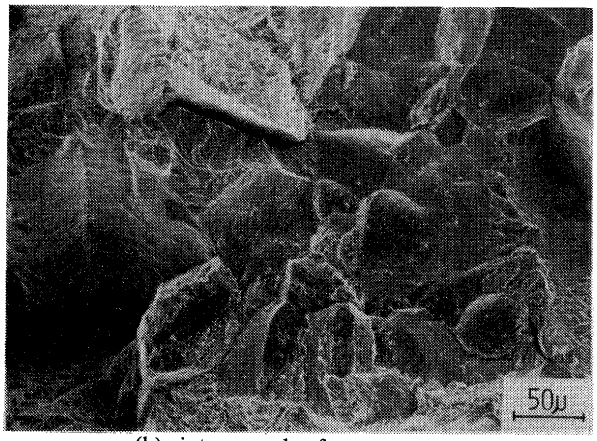

(b) intergranular fracture part

Photo. 8 Microfractograph of QC region, HY-130(E) plus E130A, $\sigma=15$ kg/mm^2, without preheating

and secondary cracks are sometimes observed but distinct river patterns seen in low temperature brittle fracture are not observed. Thus, the fracture also is considered to be resulted from hydrogen embrittlement.

Occasionally intergranular fractures which have not a directional appearance and thus are judged to occur in the heat-affected zone are observed together with the quasi-cleavage fractures as shown in **Photo. 8(b).** Because the area of the intergranular fracture is very small, they are included into the QC region.

An observation with optical microscope of the cross section of the QC region which was plated with nickel revealed that the fracture propagated along the martensite laths.

3.3.5 *D region*

The designation D is an abbreviation of dimple fracture. Macroscopically the fracture surface is dull, silky gray in appearance. In the D region, only dimple fracture is observed and the majority are equiaxed dimples as shown in **Photo. 9(a).** At the vicinities of the root edge and the bead surface,

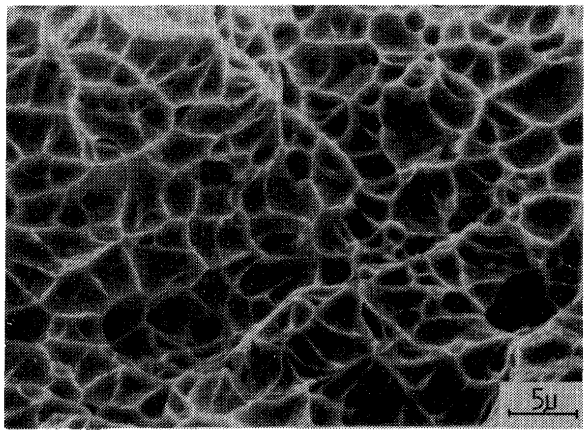

(a) equiaxed dimple, HY-130(E) plus E130A, $\sigma=$ 90 kg/mm^2, $T_p=75$ °C

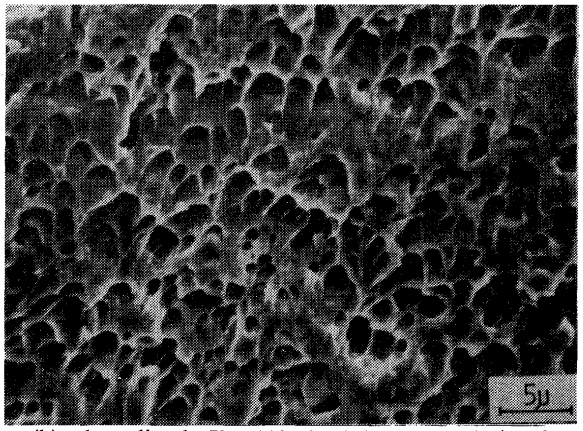

(b) shear dimple, HY-110 plus E110, $\sigma=85$ kg/mm^2 $T_p=75$ °C

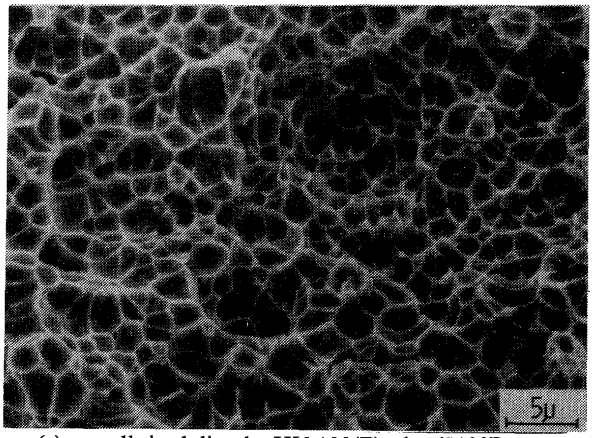

(c) small sized dimple, HY-130(E) plus E130B, $\sigma=$ 90 kg/mm^2, $T_p=75$ °C

Photo. 9 Microfractograph of D region

shear dimples shown in **Photo. 9(b)** are frequently observed. Moreover, at an extremely narrow region near the CD_c region, somewhat smaller dimples shown in **Photo. 9(c)** are observed, which may be resulted from hydrogen embrittlement according to Kikuta et al[15]. The EDX analyses of inclusions in the dimples in the combination of HY-130 (E) plus E130A show the same result as in Photo. 2(d).

This D region is considered to be unaffected by hydrogen except for the small dimple region. In other words, it is considered that the D region corresponded to a remaining portion which became unbearable against the applied load owing to the propagation of the hydrogen-induced crack and thus rapidly fractured. A similar fracture mode is reported[16] in hydrogen embrittlement of AISI4340 steel with a stress rupture test.

3.4 Distribution of Various Fracture Regions and Its Dependence on Applied Stress and Preheating Temperature

How the various fracture regions mentioned in the paragraph 3.3 are distributed on the whole of the fracture surface, and how the distribution depends on the applied stress and the preheating temperature are investigated in order to get at the characteristics of the cracking tendency of HY-130, comparing HY-130 with HY-90 and HY-110.

3.4.1 *HY*-130

(a) HY-130 (E) plus E130A (SMA welding)

The change in the fracture surface with an increase of the applied stress is shown in **Photo. 10,** where under the each macrophotograph the sketch is written with a magnification of about two times only in the direc-

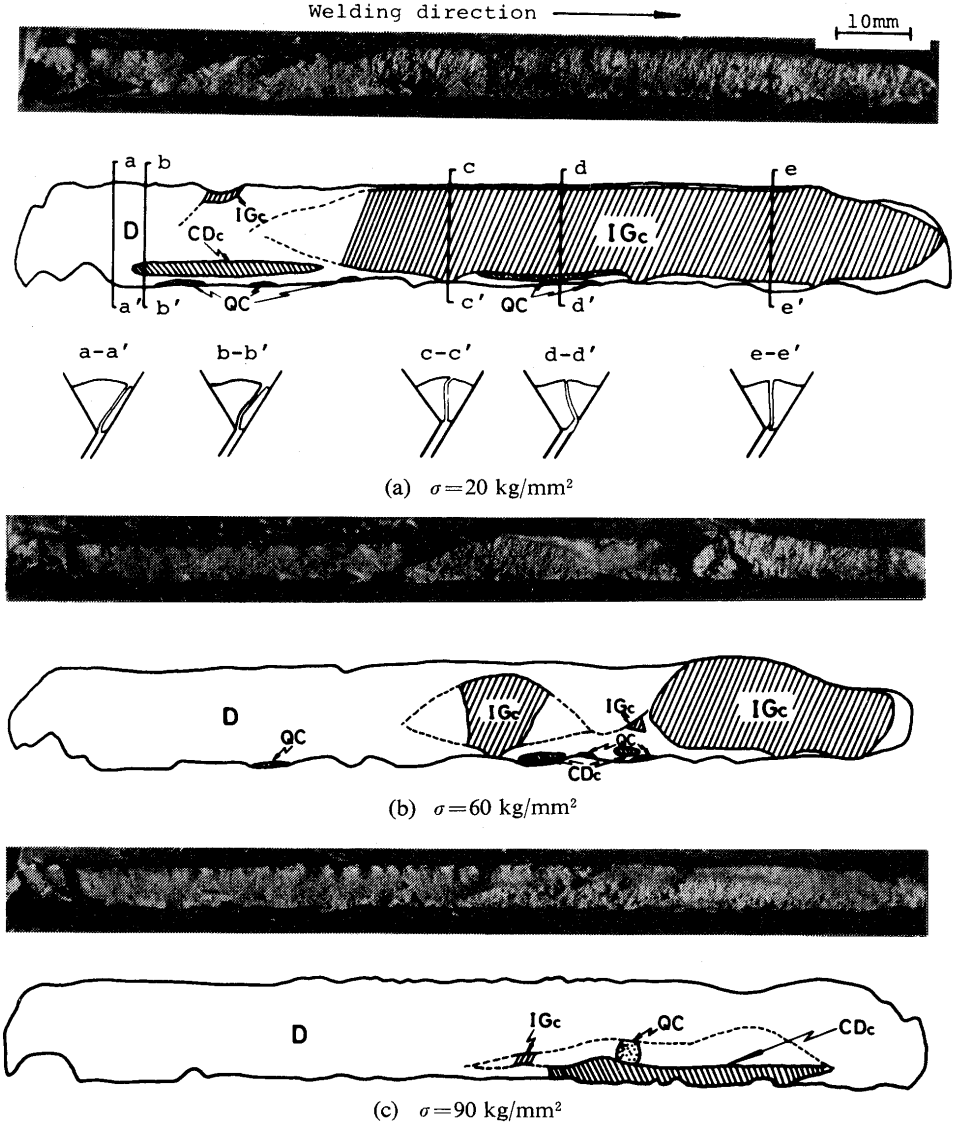

Photo. 10 Variation of light fractograph of HY-130(E) plus E130A with increase in applied stress, without preheating

tion of the throat depth. The characteristics of this combination are that at the lowest applied stress the IG_c region is remarkably dominant and that the IG_c region seems to propagate as a fan-like shape from the pivot part situated at the root edge, though the D region becomes gradually dominant in a higher applied stress. However, since it is reported[12-14] that in hydrogen-induced crack the dimple fracture is formed in the highest stress intensity factor, the D region is not considered to be the crack-initiated part of whole of the specimen. Moreover, there are few QC regions at any applied stress. These suggest that the major problem of the weld cracking of HY-130 exists in the weld metal.

Besides, in Photo. 10(a) the transverse cross section of a–a', b–b', ...and e–e' are sketched. These show that the fractures of the IG_c and CD_c regions are nearly perpendicular to the stress axis and that the fracture of the D region is not perpendicular but is roughly shear type. Photograph 1(a) and 1(b) correspond to the cross sections c–c' and b–b' respectively.

The quantitative representation of the relation between the applied stress and the area fraction of each fracture region is shown in **Fig. 2***. The increase of the applied stress decreases the IG_c region, but increases the D region. The changes in the area frac-

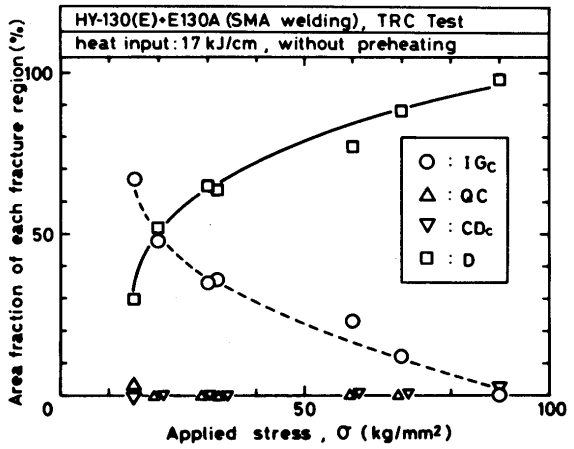

Fig. 2 Relation between applied stress and area fraction of each fracture region in HY-130 with SMA welding

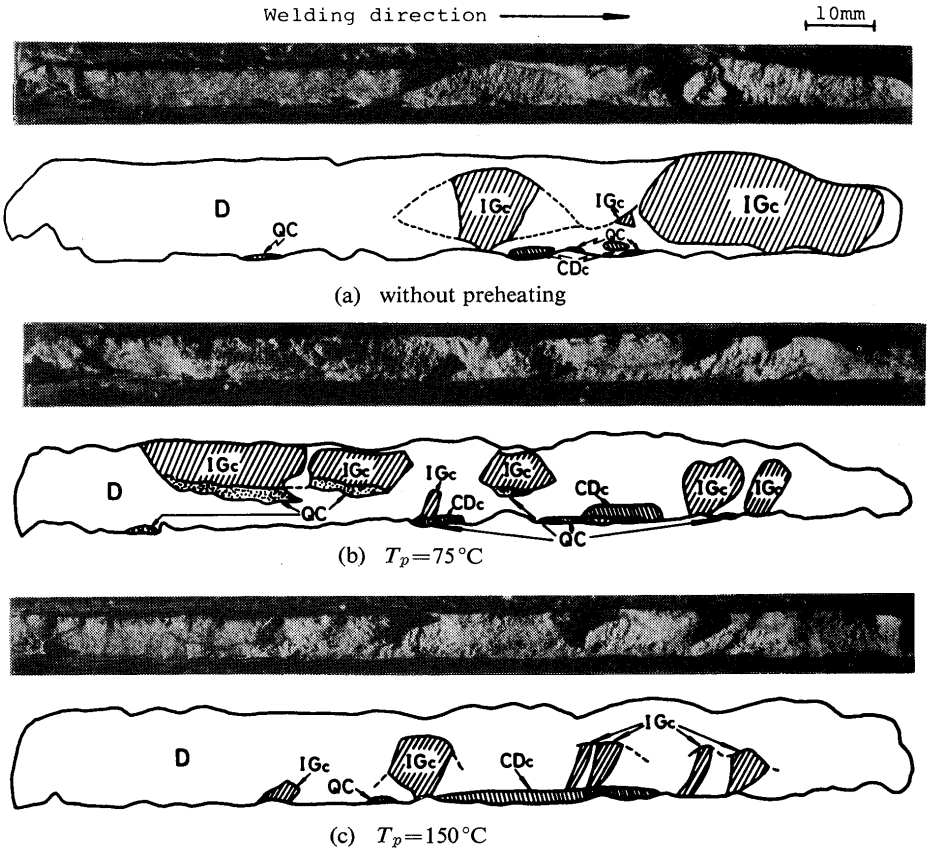

Photo. 11 Variation of light fractograph of HY-130(E) plus E130A with increase in preheating temperature, σ=60 kg/mm²

* In Figs. 2–6, data plotted on the abscissa have not zero value of area fraction, but a finite value close zero.

tions of the QC and CD_c regions are obscure owing to their few quantities. Venturing to say their tendencies, the QC region has a slightly decreasing tendency and the CD_c region has a slightly increasing tendency.

The change in the fracture surface with a rise of the preheating temperature is shown in **Photo. 11,** and the quantitative representation is shown in **Fig. 3.** The rise of the preheating temperature slightly decreases the IG_c region, but slightly increases the D region.

(b) HY-130 (F) plus F130 (GTA welding)

The change in the fracture surface with an increase of the applied stress is shown in **Photo. 12,** where the QC_c region is dominant instead of the IG_c region. Besides, crater cracks as solidification cracks are formed in both applied stresses, but there was no evidence which shows the propagation of QC_c region from the crater crack.

The increase of the applied stress decreases the QC_c region, but increases the D region as shown in **Fig. 4.**

3.4.2 *HY-90*

The change in the fracture surface with an increase of the applied stress is shown in **Photo. 13,** and the quantitative representation is shown in **Fig. 5.** The characteristics of HY-90 are that at the lowest applied stress the QC region almost occupies the vicinity of the root edge and that at a higher applied stress the D region occupies the vicinity of the root edge together with the QC region. As already mentioned, the D region is not considered to be the crack-initiated part. Therefore, the crack must initiate somewhere in the

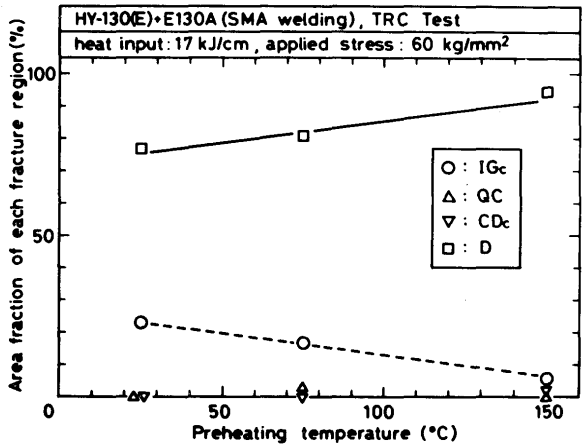

Fig. 3 Relation between preheating temperature and area fraction of each fracture region in HY-130 with SMA welding

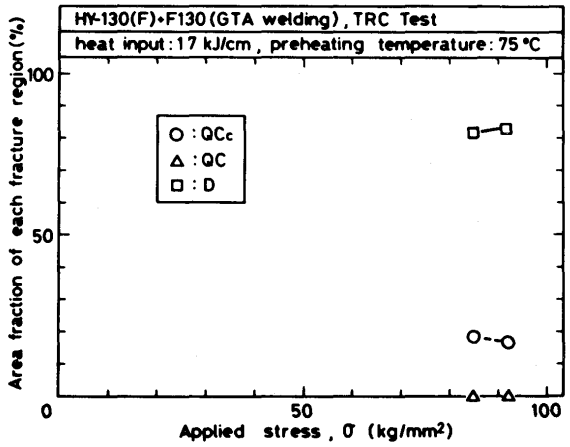

Fig. 4 Relation between applied stress and area fraction of each fracture region in HY-130 with GTA welding

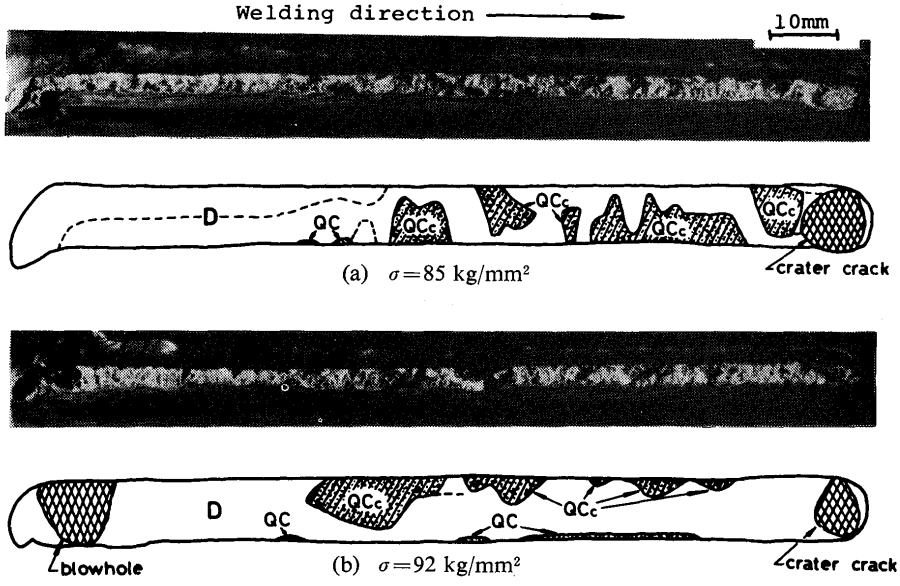

Photo. 12 Variation of light fractograph of HY-130(F) plus F130 with increase in applied stress, T_p=75 °C

QC region. Besides, according to Photo. 1(d) already mentioned, the root crack propagates from the heat-affected zone into the weld metal. Consequently the IG_c and CD_c region are observed in Photo. 13(a), but they are less than the QC region. These suggest that the major problem of the weld cracking of HY-90 exists in the heat-affected zone.

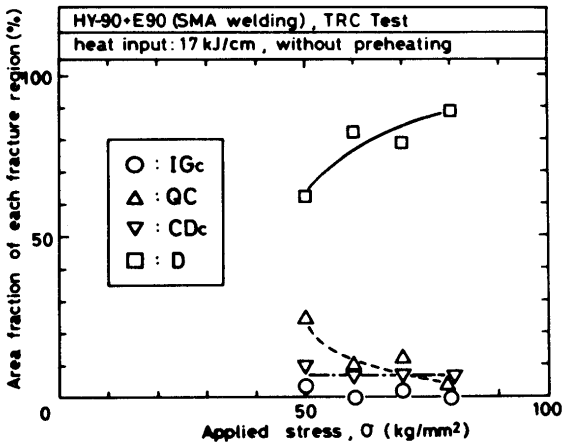

Fig. 5 Relation between applied stress and area fraction of each fracture region in HY-90

The increase of the applied stress decreases the QC region, but increases the D region as shown in Fig. 5. The IG_c and CD_c regions seem to be constant within the error range.

3.4.3 *HY*-110

The change in the fracture surface with an increase of the applied stress is shown in **Photo. 14,** and the quantitative representation is shown in **Fig. 6.** The characteristics of HY-110 are that the majority of the fracture surface somewhat resembles that of HY-90, but that there are the IG_c regions initiating at the root edge. This behavior of the IG_c region is similar to that in HY-130. In connection with this, the area fraction of the IG_c region is somewhat much than that in HY-90, and the area fraction of the QC region is less than that in HY-90. Besides, it is also observed that the area fraction of the D region increases together with the increase of the applied stress.

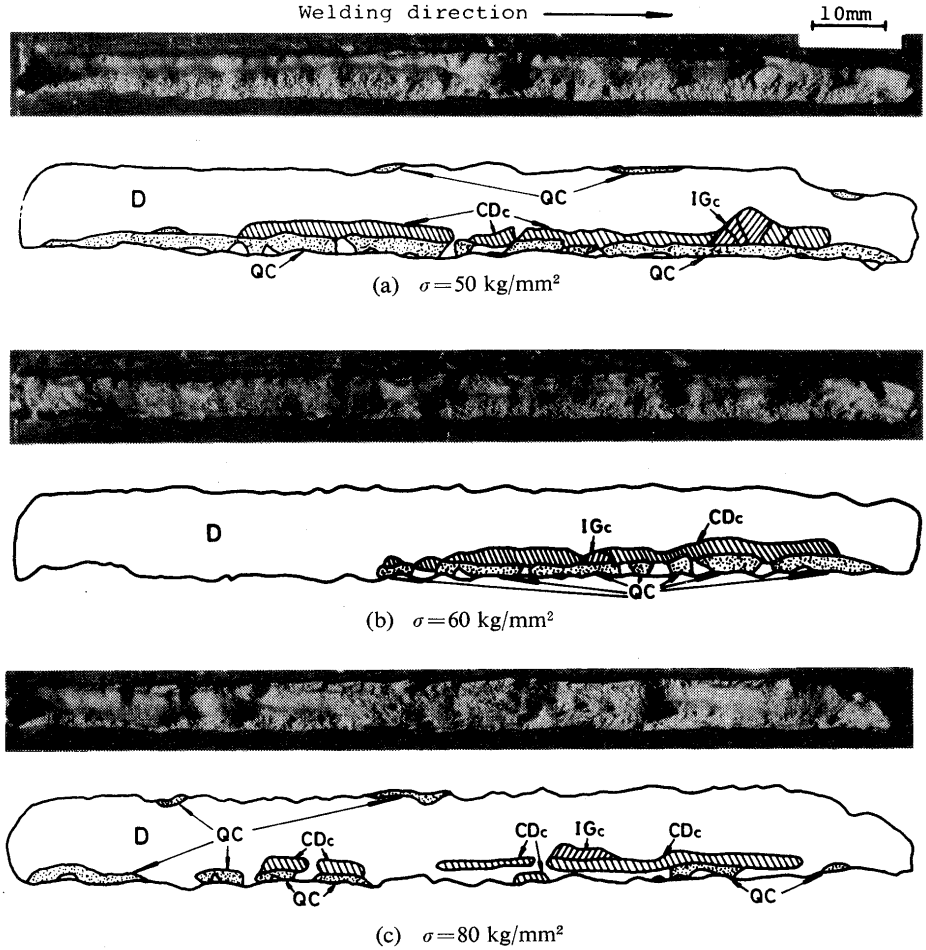

Photo. 13 Variation of light fractograph of HY-90 plus E90 with increase in applied stress, without preheating

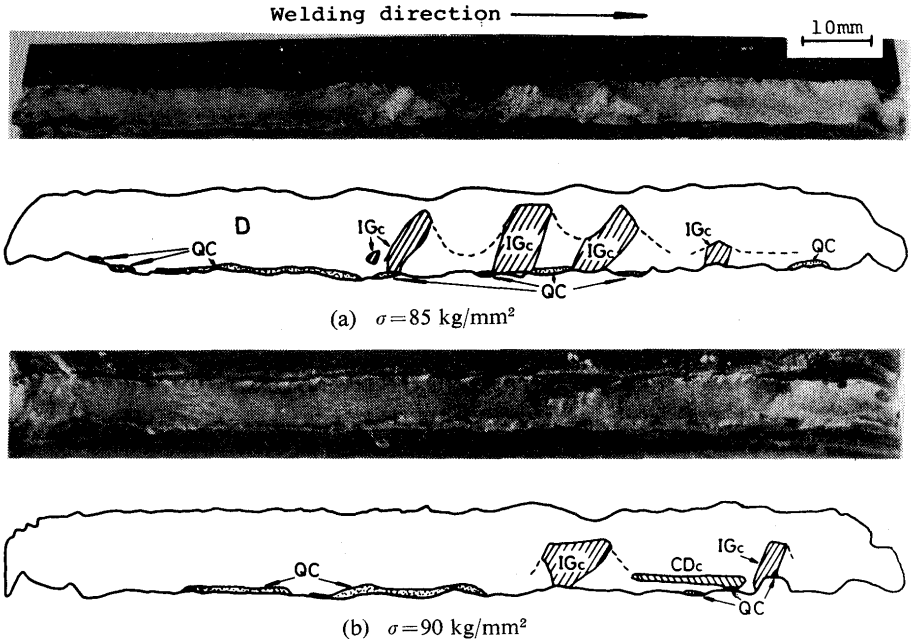

Photo. 14 Variation of light fractograph of HY-110 plus E110 with increase in applied stress, T_p=75°C

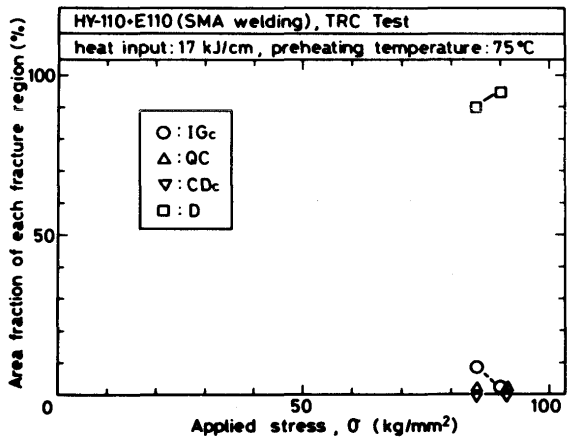

Fig. 6 Relation between applied stress and area fraction of each fracture region in HY-110

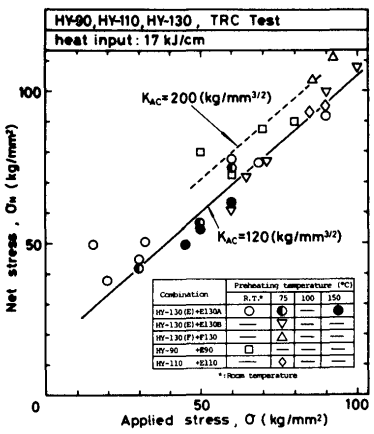

Fig. 7 Relation between applied stress and net stress at fracture

3.5 Application of Fracture Mechanics to Formation of D Region

As already mentioned in the paragraph 3.3.5, the majority of the D region are considered to be unaffected by hydrogen. In other words, it is considered that the D region corresponded to a remaining portion which became unbearable against the applied load owing to the propagation of the hydrogen-induced crack and thus rapidly fractured. Thus, one of the criterion of this fracture is that the net stress of the remaining portion becomes a critical value e.g. the tensile strength.

The net stress of the remaining portion at the fracture can be obtained by dividing the applied load by the area of the D region, and is plotted against the applies stress in **Fig. 7.** Figure 7 shows that the net stress are not constant in proportion to their levels of the tensile strength, but that the net stress increases together with the applied stress. Moreover, it is observed that the net stresses of HY-90 and HY-130 (F) plus F130 are higher than those of HY-110, HY-130 (E) plus E130A and HY-130 (E) plus E130B. These mean that the above mentioned criterion cannot be accepted.

Considering the D region from a different viewpoint, the fracture of D region is, in a sense, considered to be similar to an unstable shear crack propagation observed in the line pipes[17-19]. According to the transverse cross sections in Photo. 10(a), the fracture of the D region is shear-type as already mentioned. More-

over, the transverse cross sections suggest that the reduction of area or the elongation is macroscopically almost zero even in the D region. That is, the fracture of the D region is, so to say, macroscopically brittle, although the fracture is microscopically ductile.

These situations suggest that the linear fracture mechanics can be approximately applied to the fracture of the D region. Then, the criterion of the fracture of the D region is that the stress intensity factor increasing gradually with the propagation of the hydrogen-induced crack becomes a critical value, that is, a fracture toughness.

However, the transverse cross section of the TRC specimen is like **Fig. 8(a)**, the rigorous calculation is

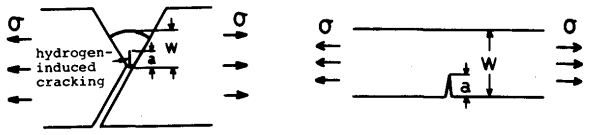

Fig. 8 Approximation of TRC specimen to single-edge-notch-specimen

difficult. Thus, the cross section of the TRC specimen is approximated to a single-edge-notch specimen shown in **Fig. 8(b)**, where σ corresponds to the applied stress, W does to the throat depth and a does to the mean depth of the hydrogen-induced crack. Then the stress intensity factor K_A is represented as*;

$$K_A = Y\sigma\sqrt{a} \qquad (1)$$

where Y is a correction factor for single-edge-notch specimen given in reference 20, which depends on a/W.

Then, the quotient obtained by dividing the difference between the total fracture area and the area of D region by the weld length gives the critical mean depth of hydrogen-induced crack. By substituting this value into Eq. (1), the K_{AC} value, which is the critical value of K_A, that is, the apparent fracture toughness can be obtained. The K_{AC} values obtained by this method are summarized in **Fig. 9**, where the K_{AC} value of each combination is roughly independent of the applied stress, although the scattering is somewhat large. The mean K_{AC} of the combination of HY-90 plus E90 is about 200 kg/mm$^{3/2}$, that of the combination of HY-110 plus E110 is about 120 kg/mm$^{3/2}$, that of the combination of HY-130 (E) plus E130A and E130B is about 120 kg/mm$^{3/2}$, and that of the combination of HY-130 (F) plus F130 is about 160 kg/mm$^{3/2}$.

Though these K_{AC} values are too small comparing

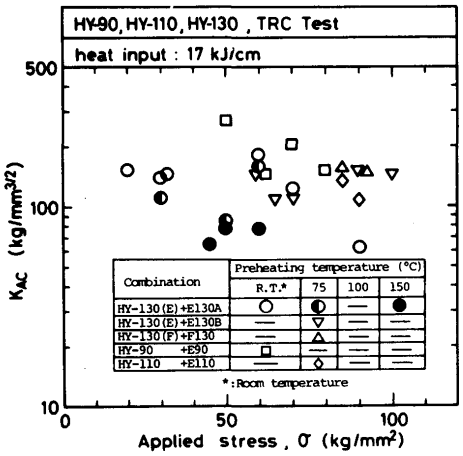

Fig. 9 Relation between applied stress and apparent fracture toughness K_{AC} of weld metal

with the usual K_{IC} values obtained in the room temperature owing to the above approximations, it is noteworthy that the ranking of the K_{AC} values agrees with that of the energy-absorption of the deposited metals in Charpy V-notch test shown in Table 2.

By the way, the area of the D region corresponding to a K_{AC} value can be obtained by the reverse calculation. The relation between the applied stress and the area fraction of the D region for K_{AC} of 120 and 200 kg/mm$^{3/2}$ is shown in Fig. 10, where the calculated results well agree with the experimental results. Moreover, the net stress at the fracture can be obtained by the reverse calculation. This is shown in Fig. 7 for K_{AC} of 120 and 200 kg/mm$^{3/2}$, where the calculated results also well agree with the experimental results.

From these discussions, it will be concluded that the D region is fractured by the unstable crack propaga-

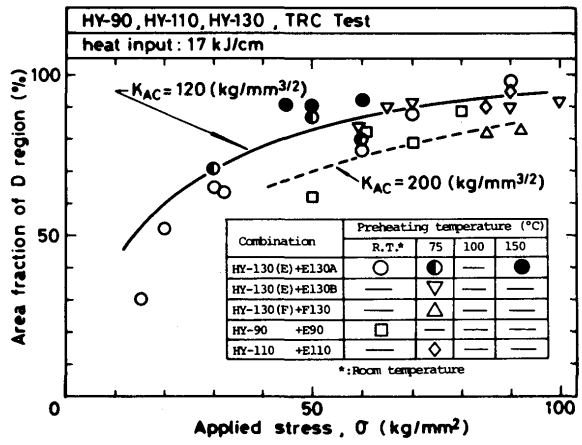

Fig. 10 Relation between applied stress and area fraction of D region

* The designation A of K_A means that the authors consider the stress intensity factor as an apparent value owing to the approximation in Fig. 8.

tion and that the linear fracture mechanics can be approximately applied to the fracture.

4. Conclusions

By observing the fracture surface of the root crack of HY-130, HY-110 and HY-90 undergone the TRC test with SEM, the clue of the weld cracking of HY-130 has been explored. Main conclusions obtained are as follows:

(1) The detailed observation revealed that the fracture surface consists of three or four fracture regions among IG_c, QC_c, CD_c, QC and D regions.

(2) The IG_c region mainly consists of intergranular fracture along columnar crystal boundary of prior austenite and partly consists of quasi-cleavage or dimple fracture. The IG_c region has a directional appearance and is formed in the weld metal. An increase of the applied stress decreases the area of IG_c region.

(3) The QC_c region mainly consists of quasi-cleavage fracture and partly consists of the same intergranular fracture as in the IG_c region. The QC_c region has a directional appearance and is formed only in the weld metal of HY-130 with GTA welding. An increase of the applied stress decreases the area of QC_c region.

(4) The CD_c region shows intermingled fracture mode of terraced quasi-cleavage fracture and dimple fracture. The CD_c region has a directional appearance and is formed in the weld metal.

(5) The QC region mainly consists of quasi-cleavage fracture and partly consists of intergranular fracture. The QC region is formed in the heat-affected zone. An increase of the applied stress decreases the area of QC region in HY-90.

(6) The D region consists of dimple fracture and is formed in the weld metal.

(7) The IG_c, QC_c, CD_c and QC regions are considered to be resulted from hydrogen-induced delayed cracking.

(8) The root crack of HY-130 with SMA welding predominantly propagates through the weld metal and contains a large quantity of IG_c region in the lowest applied stress. Therefore the crack susceptibility of the weld metal is important in HY-130. Besides, a micro solidification crack was observed near the crack-initiated parts of the IG_c region at the root edge, though there are few. However, it was considered that the micro solidification crack is not the basic cause of the weld cracking of HY-130

(9) The root crack of HY-130 with GTA welding predominantly propagates through the weld metal and the QC_c region is mainly formed. Thus there is a little intergranular fracture. It is noteworthy that the lower critical stress in GTA welding is far higher than that in SMA welding.

(10) The root crack of HY-90 propagates from the heat-affected zone into the weld metal and the QC region is dominant among the hydrogen-induced cracks in the lowest applied stress. Threefore the crack susceptibility of the heat-affected zone is important in HY-90.

(11) The majority of the D region are considered to be unaffected by hydrogen and to be fractured by an unstable crack propagation. The criterion of the fracture is that the stress intensity factor increasing gradually with the propagation of the hydrogen-induced crack becomes a critical value.

References

1) A. M. Rathbone, L. P. Connor and J. H. Gross: Weld. J., Vol. 43 (1964), 551s–563s.
2) J. H. Gross: Weld. J., Vol. 47 (1968), 241s–270s.
3) N. Bailey: Met. Const. & Brit. Weld. J., Vol. 2 (1970), pp. 339–344.
4) Y. Hirai and J. Tsuboi: J. Japan Weld. Soc., Vol. 43 (1974), pp. 366–376 (in Japanese).
5) W. F. Savage, E. F. Nippes and J. M. Sawhill: Weld. J., Vol. 55 (1976), 400s–407s.
6) H. Kihara and F. Matsuda: Trans. JWRI Vol. 2 (1973), pp. 214–224.
7) K. Masubuchi and D. C. Martin: Weld. J., Vol. 41 (1962), 375s–384s.
8) C. F. Meitzner and R. D. Stout: Weld. J., Vol. 45 (1966), 393s–400s.
9) W. F. Savage and E. S. Szeukers: Weld. J., Vol. 46 (1967), 94s–96s.
10) H. Suzuki, M. Inagaki and H. Nakamura: J. Japan Weld. Soc., Vol. 32 (1963), pp. 44–55 (in Japanese).
11) H. Kihara, H. Suzuki, M. Inagaki and H. Nakamura: J. Japan Weld. Soc., Vol. 31 (1962), pp. 53–66 (in Japanese).
12) C. D. Beachem: Met. Trans., Vol. 3 (1972), pp. 437–451.
13) F. Nakasato and F. Terasaki: Iron & Steel Inst. Japan, Vol. 61 (1975), pp. 841–855 (in Japanese).
14) F. Nakasato and F. Terasaki: Iron & Steel Inst. Japan, Vol. 61 (1975), pp. 856–868 (in Japanese).
15) Y. Kikuta, T. Araki and T. Kuroda: J. Japan Weld. Weld. Soc., Vol. 44 (1975), pp. 168–175 (in Japanese).
16) Y. Iwata, Y. Asama and A. Sakamoto: J. Japan Inst. Metals, Vol. 30 (1966), pp. 169–175 (in Japanese).
17) A. R. Duffy, G. M. McClure, R. J. Eiber and W. A. Maxey: Fracture, 1969, pp. 160–232, Academic Press.
18) G. T. Hahn, M. Szarrate, M. F. Kanninen and R. Rosenfielld: Int. J. Fracture, Vol. 9 (1973), pp. 209–222.
19) J. E. Hood and R. M. Jammieson: J. Iron & Steel Inst., Vol. 211 (1973), pp. 369–373.
20) B. Gross, J. E. Srawley and W. F. Brown: NASA TN, D-2395, 1964, pp. 1–14.